

# Creep behaviour of a parallel-lay aramid rope

G. B. GUIMARÃES

*Departamento Engenharia Civil, Pontificia Universidade Católica do Rio de Janeiro, Rua Marquês de São Vicente 225, 22453 Rio de Janeiro, Brazil*

C. J. BURGOYNE

*Engineering Department, Cambridge University, Trumpington Street, Cambridge CB2 1PZ, UK*

A series of dead load tests on a parallel-lay aramid rope has been conducted with the purpose of studying its creep behaviour. The main variable considered in the tests was the applied stress which varied from 24.5%–81.6% ultimate tensile strength. It was found that creep and recovery are adequately described by a logarithmic time law and that the creep coefficient for the material can be considered stress independent. An empirical expression for prediction of long-term creep at ambient temperature is presented.

## 1. Introduction

The remarkable progress in the polymer industry over the last decades has produced new materials with revolutionary mechanical properties. One example is the high-strength high-modulus aramid fibre Kevlar\*, which has already found wide application in composites in situations where weight is of fundamental importance, as in the aerospace industry.

This fibre is also being used in the manufacture of cables and ropes which are of interest for structural applications as tension members. Among the three basic constructions of fibre ropes, twisted, braided and parallel-lay, the latter has the highest strength, highest modulus and best fatigue performance achievable with a particular fibre. A range of this type of rope, known as Parafil†, is currently manufactured by Linear Composites Ltd, with Type G being the version with the highest elastic modulus and tensile strength. This rope consists of a core of parallel and continuous Kevlar 49 yarns encased by a polymeric sheath which maintains the circular profile of the rope and protects the core from abrasion and ultraviolet light. Type G Parafil has a linear stress–strain relationship with a nominal strength of  $1926 \text{ kN mm}^{-2}$  and a strain at failure of about 1.5%. Earlier work [1] had indicated that stress rupture can be described by a linear relationship between load and logarithm of time to break; when subjected to loads equivalent to 64% and 50% of the nominal breaking load, for instance, the lifetimes of the material are 1 and 100 years, respectively.

Type G Parafil ropes have been identified as an attractive material for use in prestressed concrete structures, cable stayed and suspension bridges, cable supported roofs [2] and in tension leg platforms [3, 4]. It is clear that for these applications a good understanding of the creep properties of the material is

highly desirable, because load durations of many decades are required.

The present investigation is concerned with the creep and stress-rupture properties of Type G Parafil over periods extending to years. The tests were carried out at Imperial College in London, on specimens subjected to constant and varying loads at ambient temperature. A discussion on the creep behaviour of the ropes is given here while the stress-rupture results are analysed separately [5].

## 2. Test programme

### 2.1. Specimens

The specimens used in this study were 1.5 tonne and 3.0 tonne Type G Parafil ropes, with cross-sectional area of the yarn in the core of 7.64 and 15.28 mm<sup>2</sup>, respectively. They were anchored with standard spike and cone terminals supplied by the manufacturer; these have proved to be capable of anchoring the full strength of the rope [1]. The length of all creep specimens was 2 m (from tip to tip of the spikes within terminals). Their tensile strengths, obtained from short-duration tests of 1.5 m long specimens, are shown in Table I. The tensile tests were carried out in an Amsler hydraulic machine at a loading rate of 7 kN min<sup>-1</sup>.

### 2.2. Creep tests under constant load

Table II shows the number of specimens tested under constant loads with the corresponding stress levels. Before starting the tests, all specimens were pre-tensioned to the loads given in the table. The procedure of

\* Kevlar is a trade name of EI Du Pont de Nemours.

† Parafil is a trade name of Linear Composites Ltd.

TABLE I Tensile strength of the specimens

	Specimen no.	Load (kN)	Strength (MPa)
1.5 tonne ropes	1	17.75	2323
	2	18.54	2426
	3	18.24	2388
	4	17.75	2323
	5	19.03	2490
	6	18.83	2465
			Mean 2403
3 tonne ropes	1	33.69	2205
	2	34.28	2243
	3	33.54	2195
	4	34.23	2240
	5	32.36	2118
	6	33.54	2195
			Mean 2200

applying a pretensioning load has the effect of eliminating any possible initial disorientation of the fibre lay which is caused by the coiling process (Parafil ropes are supplied in circular drums, diameter =  $50 \times$  rope diameter). Following the application of the pretensioning loads, which took less than 1 min, the ropes were unloaded and a time for recovery (around 5 min) was allowed before starting the test.

The pretensioning load was 60% of the nominal breaking load, for those specimens tested under loads below this value, and of the same magnitude as the test load for those tested beyond 60% of nominal breaking

load. Two measures of rope capacity will be used. Nominal breaking load (NBL) is the manufacturer's rated capacity of the rope, based on a uniform stress of  $1926 \text{ kN mm}^{-2}$ , irrespective of area. The actual breaking load (ABL) is higher than this, and varies slightly with area (when expressed as a stress) due to the effects of bundle theory. ABL is found to give better correlations between ropes of different sizes, for both creep and stress-rupture data, than NBL.

Table II shows that the range of the applied load varied from 24.5%–81.6% of the ABL of the specimens. Specimens tested at loads above 60% ABL were expected to be loaded until they failed by stress-rupture, but creep data could be obtained from all tests since the test methods were identical.

### 2.3. Creep tests under varying load

Three tests were carried out under varying loads. The stress levels and their corresponding duration for each specimen are given in Table III. All three specimens were pretensioned to the maximum value of the loading programme (77% ABL) following the same procedure as in the previous section. The first loading stage consisted of the application of a given load for 1 day. This load was then removed and the specimen was left unloaded for 2 days. In the following stages, each with 1 week duration, the load was gradually increased up to 77% ABL after which the load was kept constant until failure of the specimen.

TABLE II Specimens tested under constant loads

	Specimen	Pretension (kN)	Creep load (kN)	Stress (MPa)	% NBL <sup>a</sup>	% ABL <sup>b</sup>
3 tonne ropes	C93-1	27.43	27.43	1795	93.2	81.6
	C93-2	27.43	27.43	1795	93.2	81.6
	C93-5	27.43	27.43	1795	93.2	81.6
	C93-6	27.43	27.43	1795	93.2	81.6
	C93-7	27.43	27.43	1795	93.2	81.6
	C93-8	27.43	27.43	1795	93.2	81.6
	C87-1	25.49	25.49	1668	86.6	75.8
	C87-2	25.49	25.49	1668	86.6	75.8
	C87-3	25.49	25.49	1668	86.6	75.8
	C87-5	25.49	25.49	1668	86.6	75.8
	C87-6	25.93	25.93	1697	88.1	77.1
	C87-7	25.49	25.49	1668	86.6	75.8
	C87-8	25.93	25.93	1697	88.1	77.1
	C82-1	24.16	24.16	1581	82.1	71.9
	C76-1	22.45	22.45	1469	76.3	66.8
	C72-1	21.22	21.22	1389	72.1	63.1
	C65-1	19.25	19.25	1260	65.4	57.3
	C50-1	17.66	14.68	961	50.0	43.7
	C40-1	17.66	11.76	770	40.0	35.0
	1.5 tonne ropes	R91-1	13.46	13.46	1762	91.5
R91-2		13.46	13.46	1762	91.5	73.3
R91-3		13.46	13.46	1762	91.5	73.3
R91-4		13.43	13.43	1757	91.3	73.1
R91-5		13.43	13.43	1757	91.3	73.1
R91-6		13.46	13.46	1762	91.5	73.3
R85-1		12.44	12.44	1629	84.6	67.8
R85-2		12.42	12.42	1625	84.4	67.6
R80-1		11.77	11.77	1540	80.0	64.1
R30-1		8.70	4.49	588	30.5	24.5

<sup>a</sup> % NBL: percentage of nominal breaking load.

<sup>b</sup> % ABL: percentage of actual breaking load.

TABLE III Specimens tested under varying loads

Stage	Specimen VR1		Specimen VR2		Specimen VR3	
	Duration (day)	Load (%ABL)	Duration (day)	Load (%ABL)	Duration (day)	Load (%ABL)
1st	1.02	57.0	1.01	47.4	1.00	38.0
2nd	1.98	0.0	1.96	0.0	2.03	0.0
3rd	6.99	57.0	7.02	47.4	6.97	38.0
4th	7.00	65.0	7.00	57.0	6.99	47.4
5th	7.00	73.0	7.15	65.0	7.03	57.0
6th	9.35 <sup>a</sup>	77.0	7.04	73.0	7.05	65.0
7th	-	-	5.82 <sup>a</sup>	77.0	6.90	73.0
8th	-	-	-	-	8.49 <sup>a</sup>	77.0

<sup>a</sup> Until failure

Pretension: 77% ABL for all specimens.

Specimens: 1.5 tonne Type G Parafil ropes.

### 2.4. Test rig and instrumentation

The tests were carried out in modular rigs using dead weight loading with a 10:1 level arrangement (Fig. 1). The load was transmitted to the ropes through two perpendicular pins, placed at both ends of the rope, which allowed free rotations at those points, preventing local bending of the rope. Rope extensions were measured with linear variable differential transformers (LVDTs), monitored with a data acquisition system, which gave the relative displacement between the terminals. Dial gauges were used to measure the spike bed-down which was taken into account to obtain the net extension.

The precision of the strain measurements was  $\pm 10 \times 10^{-6}$  for the 1.5 tonne rigs and  $\pm 4 \times 10^{-6}$  for the 3 tonne rigs at the 90% confidence limit (the LVDTs used in the 3 tonne rigs were more sensitive than those used in the 1.5 tonne rigs).

## 3. Test results

### 3.1. Creep strains

The general form of the creep curves is shown in Fig. 2 for the specimens tested under constant load. This curve is characteristic of most materials, depending on the test conditions, such as applied stress and temperature. The curve is divided into three stages corresponding to primary, secondary and tertiary creep. The creep rate, which is fairly large in the first stage, gradually decreases becoming a minimum during the secondary creep stage. The third stage is characterized by a sudden increase of the creep rate and terminates in failure. Fig. 3 shows two typical results with these three stages well defined while the third test did not fail. Fig. 4 shows the strain responses and corresponding loading programme for the specimens tested under time-varying loads.

### 3.2. Creep strain representation and creep rate

The strain data are shown in Figs 5–11 against logarithm of time. These figures show that the relationship between strain and logarithm of time is linear for primary and secondary creep stages, indicating

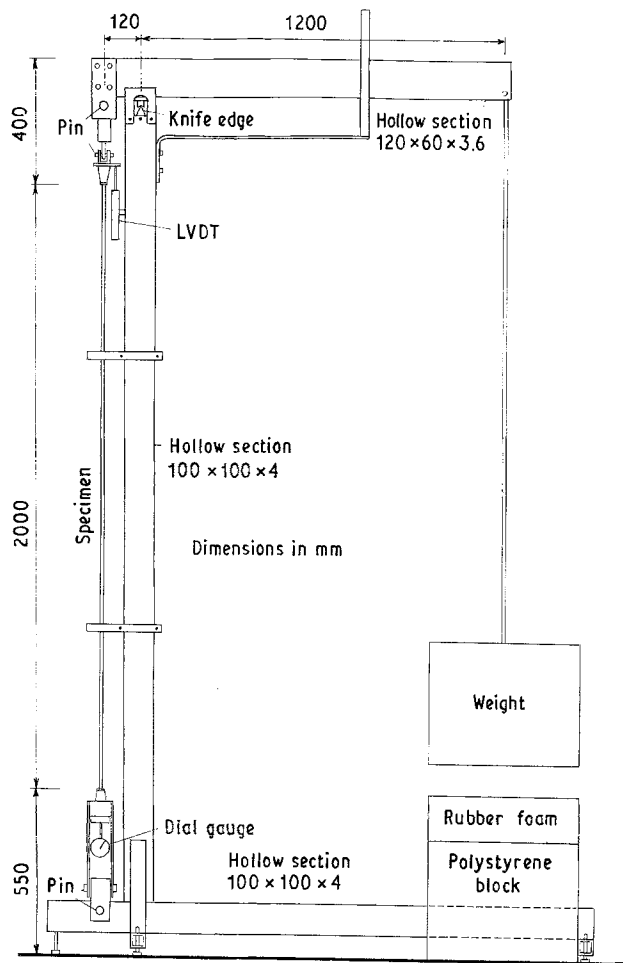


Figure 1 Details of 3 tonne rigs.

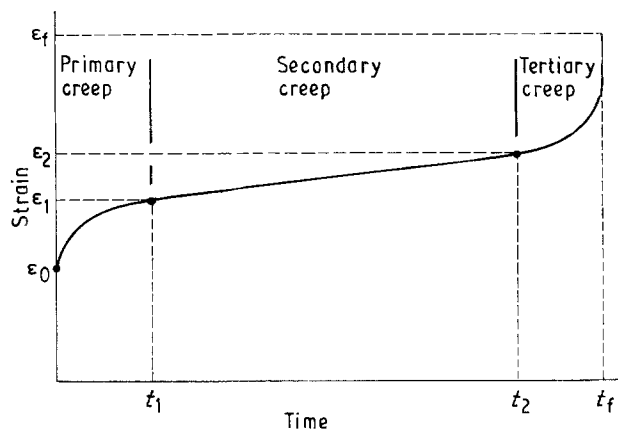


Figure 2 Creep curve.

that the strain–time behaviour of these parallel-lay ropes can be described by an expression of the form

$$\epsilon(t) = \beta \log_{10}(t) + \epsilon_1 \quad t > 0 \quad (1)$$

This expression has the disadvantage that at time zero the strain would be minus infinity, but it is clear from the figures that this expression can be used at all practical time values (say from 1 s). In this logarithmic expression, the constant  $\epsilon_1$  is the strain value at unit time and the slope  $\beta$  (creep rate parameter) is related to the creep rate  $d\epsilon(t)/dt$  by

$$d\epsilon(t)/dt = \beta/2.3t \quad (2)$$

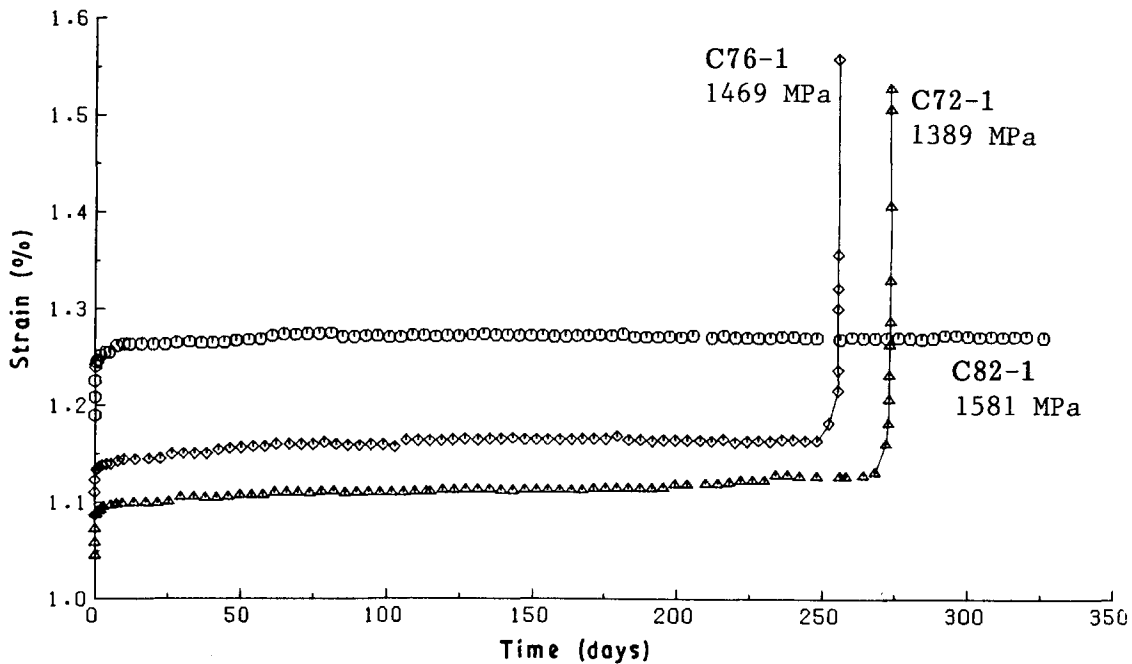


Figure 3 Typical creep test results.

The values given in Table IV for the creep rate parameter,  $\beta$ , were obtained by linear regression analysis. The relationship between the creep rate parameter and the initial strain is shown in Fig. 12, which indicates that  $\beta$  increases with applied stress.

### 3.3. Times to break

The times to break,  $t_b$ , observed in the constant-load tests are shown in Table IV. The stress versus logarithm of lifetime plot is shown in Fig. 13. These results are analysed in detail in Reference 5.

### 3.4. Creep capacity

Creep capacity is here defined as the difference between the strain at the end of the secondary creep stage and the initial strain ( $\epsilon_2$  and  $\epsilon_0$  in Fig. 2, respectively). Table IV gives the values of creep capacity for all the specimens and Fig. 14 shows the relationship between this parameter and applied stress. A wide scatter is observed but it seems that creep capacity is independent of stress.

### 3.5. Mode of failure

The mode of failure observed in the tensile (Section 2.1) and stress-rupture tests was characterized by the rupture of the yarns at different positions along the length of the specimens. In a few stress-rupture specimens, 20–30% of the yarns failed in a section close to one of the terminals.

## 4. Discussion

### 4.1. Stress dependence of the creep coefficient for Parafil

One way of studying the stress dependence of the creep behaviour of a material is by using the iso-

chronous curves (stress versus creep strain curves for a constant time) which provide a simple check of the linearity, or non-linearity, of the material. An alternative way is by studying the coefficients of the mathematical expressions found to represent the creep coefficient of the specimens tested at different stresses, which is adopted here.

The creep coefficient,  $\phi(t)$ , is defined as the ratio of the creep strain,  $\epsilon_c(t)$ , to the initial strain,  $\epsilon_0$ , i.e.

$$\begin{aligned} \phi(t) &= \epsilon_c(t)/\epsilon_0 \\ &= [\epsilon(t) - \epsilon_0]/\epsilon_0 \end{aligned} \quad (3)$$

where  $\epsilon(t)$  is the total strain at time  $t$ . If the unit time is taken as 1 s, the corresponding strain,  $\epsilon_1$ , in Equation 1 can be considered as the initial strain. This is reasonable because the choice of the time at which creep is considered to be zero is arbitrary because the load cannot be applied instantaneously. Thus, the expression for the creep coefficient can be written as

$$\phi(t) = \frac{\beta}{\epsilon_0} \log_{10}(t) \quad (4)$$

With the values of the creep rate parameter,  $\beta$ , and the initial strain,  $\epsilon_0$ , values given in Table IV, the ratio  $\beta/\epsilon_0$  (creep coefficient parameter) for each specimen can be calculated. Their values are given in the last column of the table and plotted against applied stress in Fig. 15.

It is already known that the operating stress of parallel-lay ropes will be governed by their stress-rupture properties [6]. In the great majority of practical situations, the operating stress would not exceed 1200 MPa, which represents approximately 60% of the static strength, and therefore the stress range of interest for the study of the viscoelastic properties, from a practical point of view, should be limited by the above value. It is instructive, however, to consider all the available data in order to identify any particular

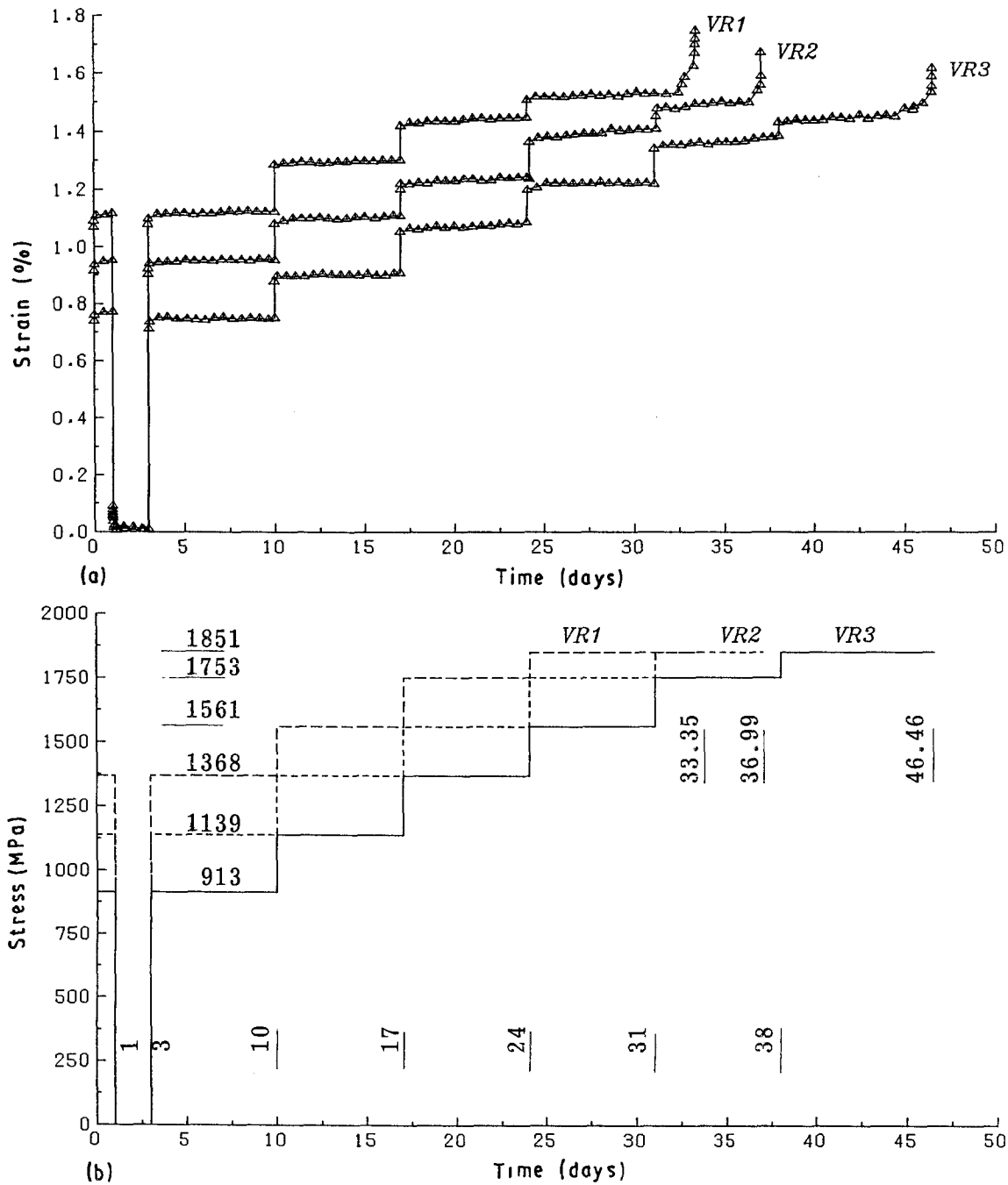


Figure 4 Results of varying load creep tests. (a) Strain response, (b) loading programme.

trend in creep behaviour. If, for instance, only the few data points below 1200 MPa in Fig. 15 are considered, a decrease of the creep coefficient parameter,  $\beta/\epsilon_0$ , with increasing stress would be suggested. The points beyond 1200 MPa, on the other hand, indicate that this trend could be masked by the scatter of the data.

In the absence of additional experimental data at lower stresses, it will be assumed, at this stage, that the creep coefficient parameter,  $\beta/\epsilon_0$ , is independent of stress. In this case, the best representation for it is the mean of the values given in Table IV, which is 0.012/decade. (This is equivalent to assuming a linear relationship between the creep rate parameter,  $\beta$ , and the initial strain,  $\epsilon_0$ , or applied stress, in Fig. 12). Confidence limits can be assigned to this value by choosing a statistical distribution for the data points. Fig. 16 shows that the normal distribution is adequate

and, thus, the confidence limits can be obtained by multiplying the standard deviation, which was found to be 0.0017, by a factor which depends on the desired probability. For 90% certainty this factor is 1.645 which leads to the limits  $\pm 0.003$ . The numerical expression for estimating the creep coefficient of the ropes can now be written, with  $t$  (s) as

$$\phi(t) = (0.012 \pm 0.003) \log_{10}(t) \quad (5)$$

#### 4.2. Creep recovery

The creep and recovery data for the three specimens VR1, VR2 and VR3 (see Section 2.3), tested under different stresses, are shown in Table V for a 1 day recovery period which followed the 1 day creep period. The comparison between the total strain after 1 day

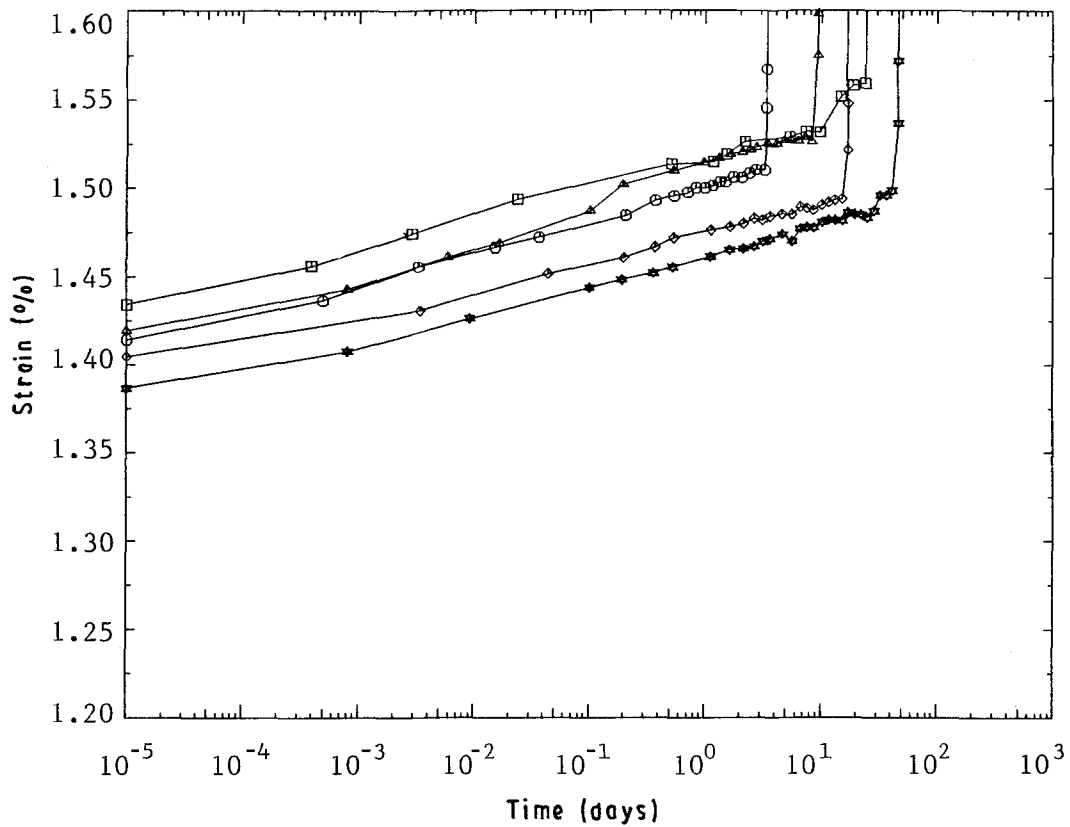


Figure 5 Strain versus logarithm of time (1.5 tonne ropes). (□) R91-2, (○) R91-3, (△) R91-4, (◇) R91-5, (☆) R91-6.

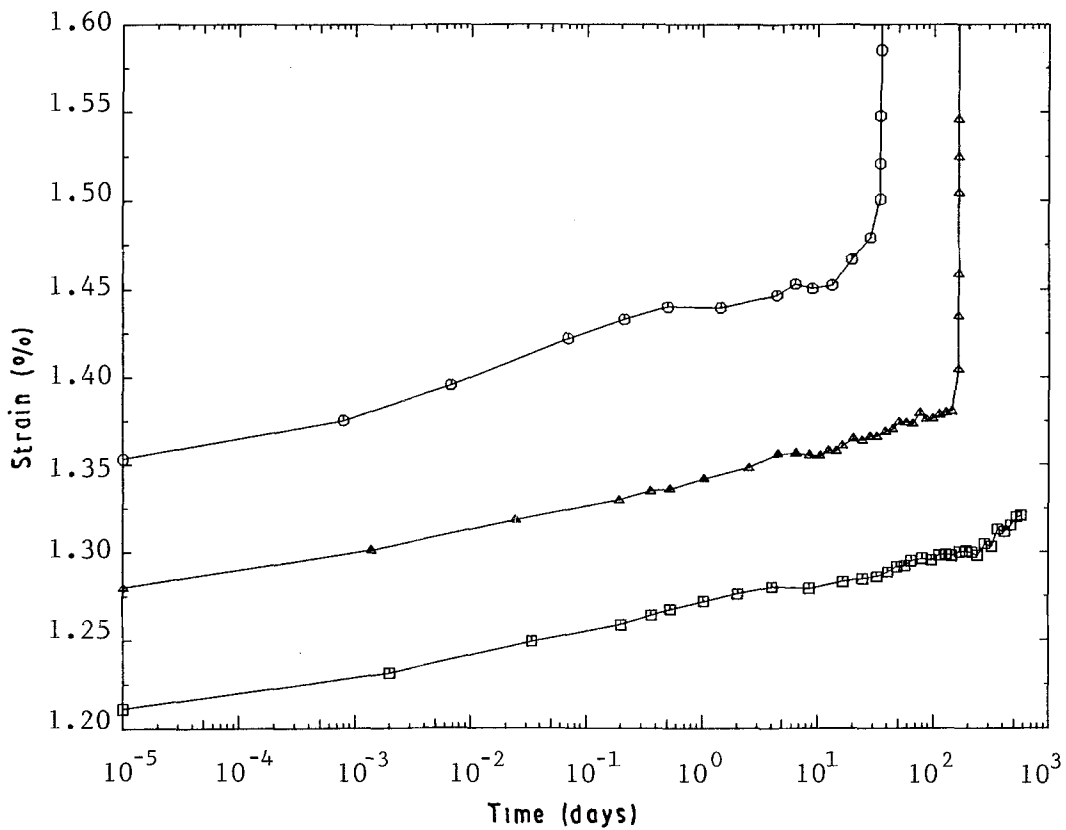


Figure 6 Strain versus logarithm of time (1.5 tonne ropes), (□) R80-1, (○) R85-1, (△) R85-2.

and the total recovery in the following day (last column of the table) indicates that an almost complete recovery took place. The comparison between the initial strain and the initial strain recovery, however, shows that the latter amounted to 94–97% of the

initial strain. This is equivalent to an increase in the elastic modulus upon unloading as shown in Table VI. As the specimens were loaded again to the previous levels, after the 2 day recovery period, the modulus values were less than those observed upon unloading,

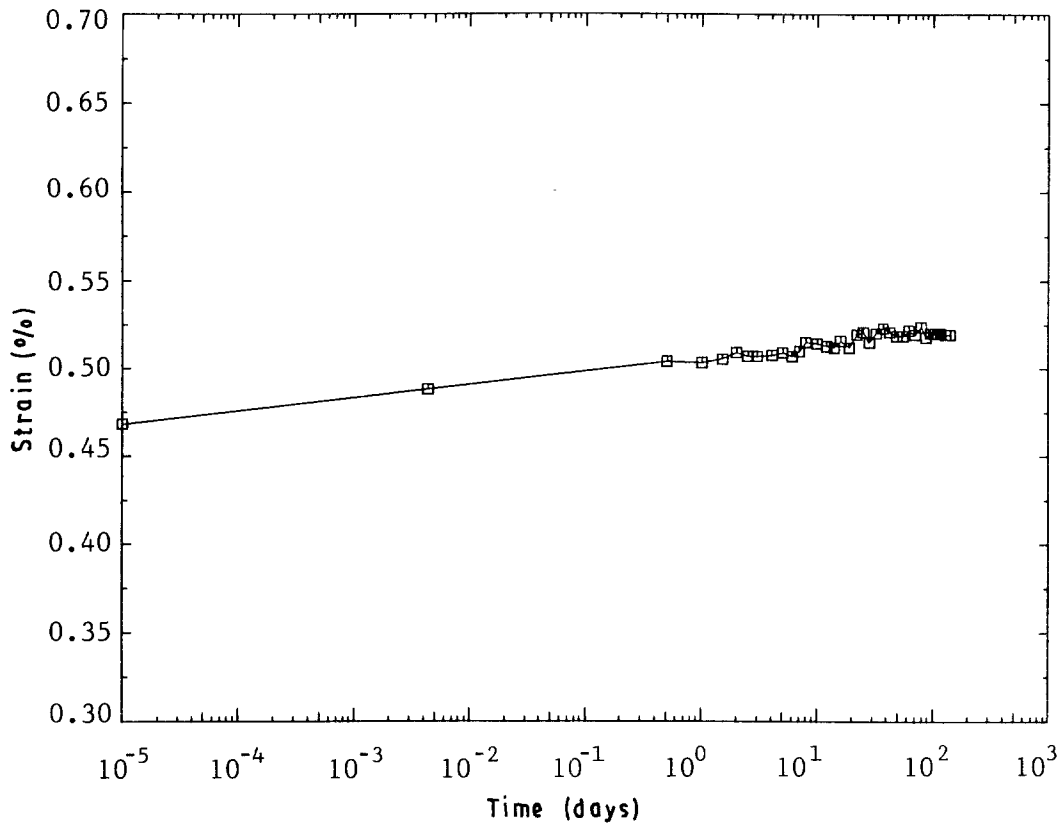


Figure 7 Strain versus logarithm of time (1.5 tonne ropes), for R30-1.

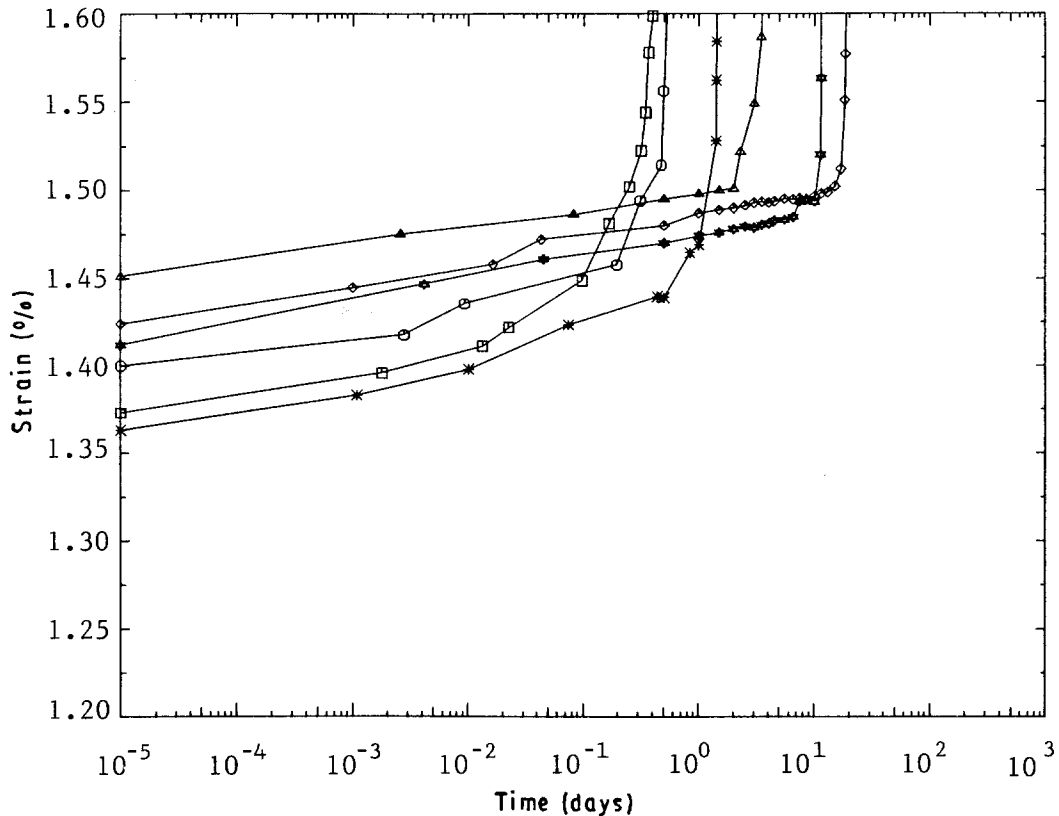


Figure 8 Strain versus logarithm of time (3 tonne ropes). ( $\square$ ) C93-1, ( $\circ$ ) C93-2, ( $\triangle$ ) C93-5, ( $\diamond$ ) C93-6, ( $*$ ) C93-7, ( $\star$ ) C93-8.

but slightly greater than the values measured in the first stage, as shown in Table VI. These differences on loading and unloading behaviour might, however, be attributed to different loading/unloading rates, which were not controlled in the tests.

The creep and recovery data corresponding to the first and second stages of the experiments (see Table III) are plotted in Fig. 17 which shows that recovery strain, like creep, is linearly related to logarithm of time. The figure also shows that the slope of the

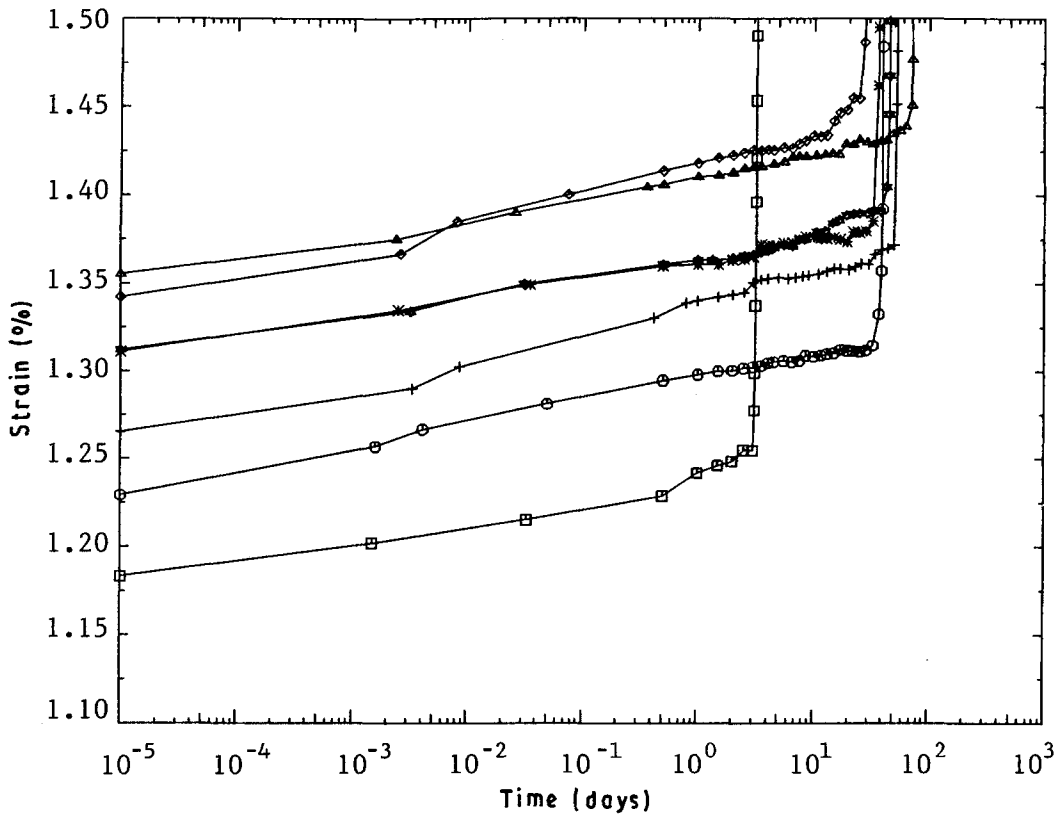


Figure 9 Strain versus logarithm of time (3 tonne ropes). ( $\square$ ) C87-1, ( $\circ$ ) C87-2, ( $\triangle$ ) C87-3, ( $\diamond$ ) C87-5, ( $*$ ) C87-6, ( $\star$ ) C87-7, ( $+$ ) C87-8.

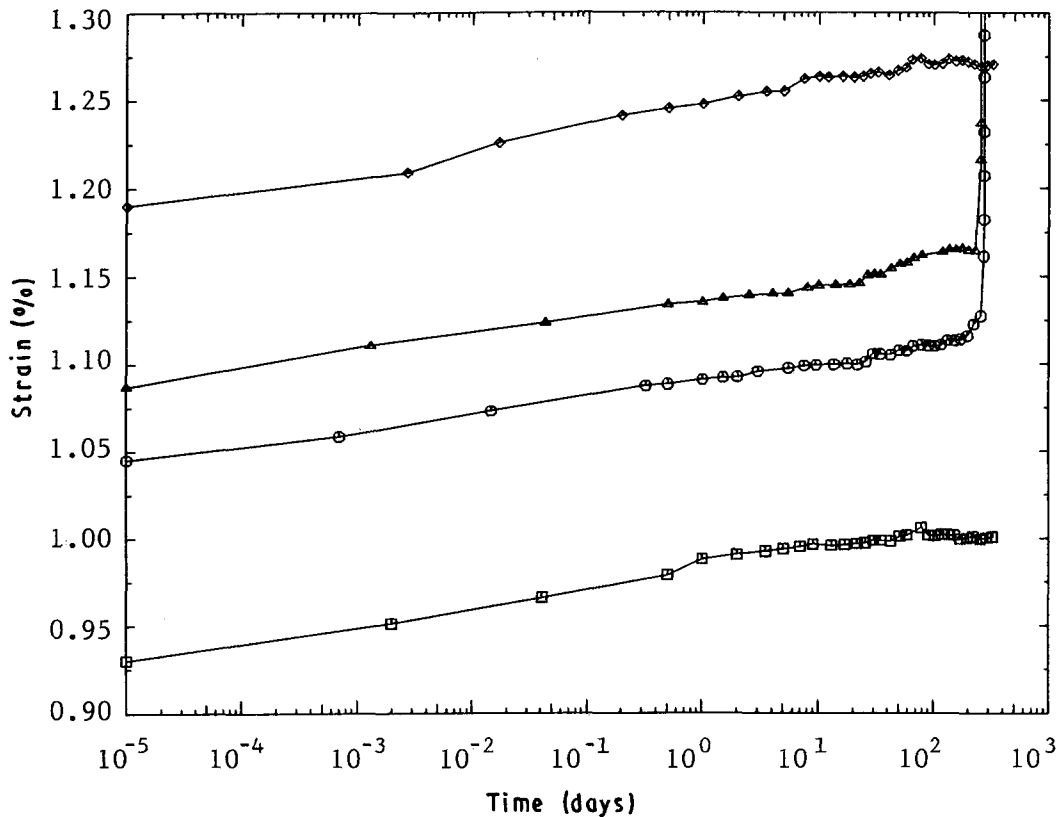


Figure 10 Strain versus logarithm of time (3 tonne ropes). ( $\square$ ) C65-1, ( $\circ$ ) C72-1, ( $\triangle$ ) C76-1, ( $\diamond$ ) C82-1.

recovery lines are greater than those corresponding to creep, for all specimens, indicating that the recovery rate was greater than the creep rate. The values of the slopes, obtained by a regression analysis, are given in Table VII.

## 5. Comparisons with earlier work

### 5.1. Functional form for the creep law

The logarithmic representation adopted here, and also for other tests on 60 tonne ropes [6], to represent the creep strain of parallel-lay aramid ropes, seems to be



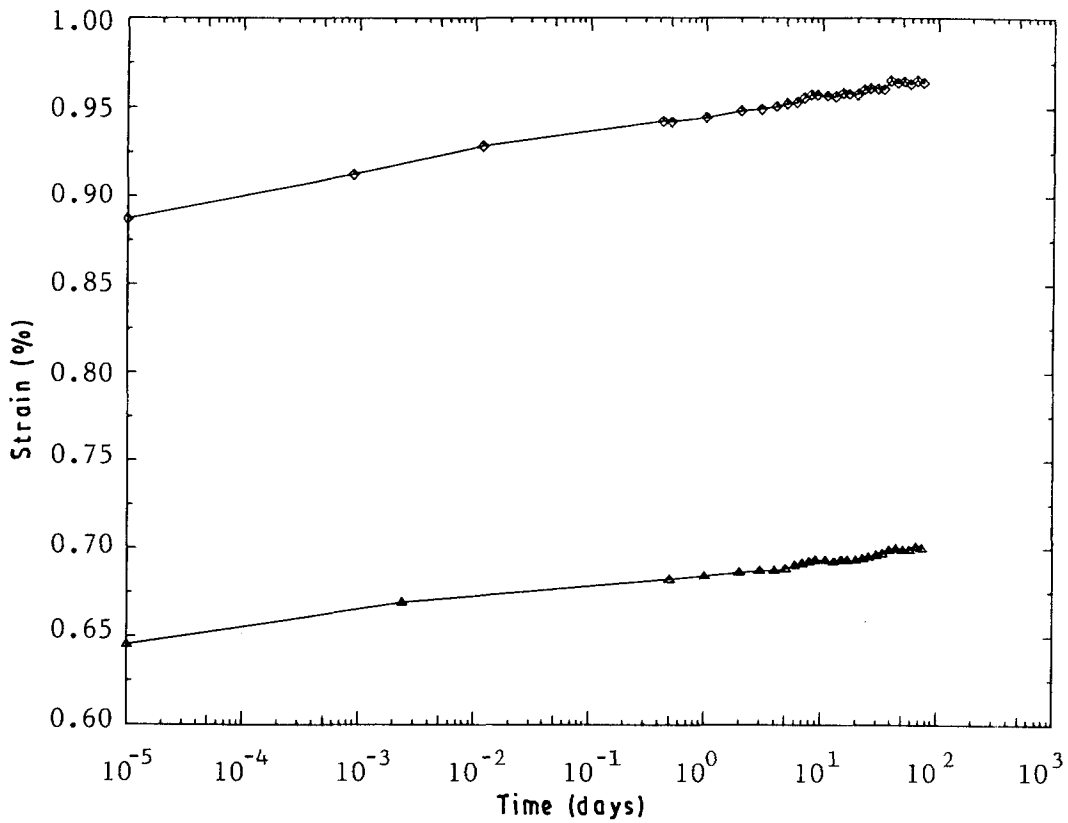


Figure 11 Strain versus logarithm of time (3 tonne ropes). ( $\Delta$ ) C40-1, ( $\diamond$ ) C50-1.

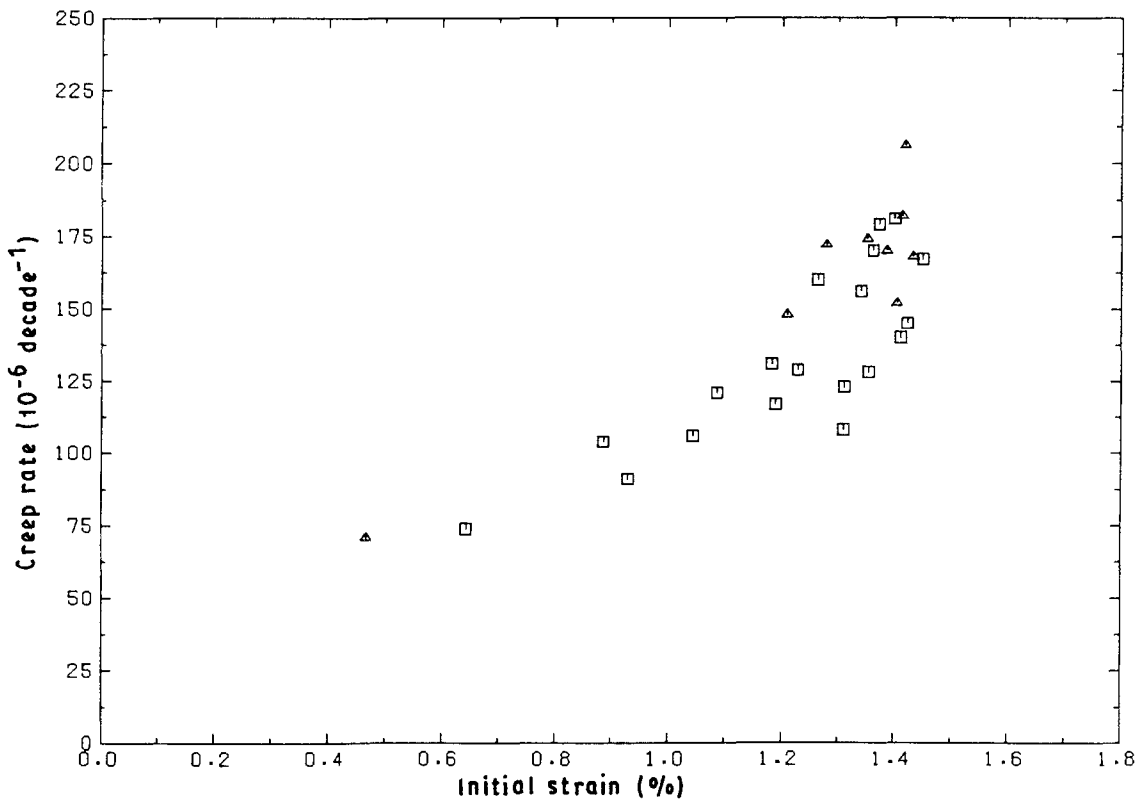


Figure 12 Creep rate parameter versus initial strain, for ( $\Delta$ ) 1.5 tonne and ( $\square$ ) 3 tonne ropes.

the most widely used for Kevlar. The linearity between creep strain and logarithm of time has been observed for Kevlar 49 yarns over a period exceeding 1 year [7, 8] and for Kevlar 49 filaments over periods up to 1000 h [9, 10]. In both cases a logarithmic time law was found adequate for creep recovery as well. Schaefer

[11] reported that H Blades (in a private communication) also modelled the creep behaviour of Kevlar 49 using a logarithmic time law. Walton and Majumdar [12], on the other hand, used a power law to model the creep behaviour of Kevlar filaments over a period exceeding 4 years.

TABLE IV Results of constant-load creep tests

Specimen	$\sigma$ (MPa)	% ABL	$\epsilon_0$ (%)	$E = \sigma/\epsilon_0$ (MPa)	$t_b$ (day)	$\beta$ ( $10^{-6}$ decade $^{-1}$ )	Correlation coeff. for $\beta$	$\epsilon_2$ (%)	$\epsilon_2 - \epsilon_0$ (%)	$\beta/\epsilon_0$ (decade $^{-1}$ )
3 tonne ropes										
C93-1	1795	81.6	1.373	130 736	0.418	179	0.936	1.481	0.108	0.0130
C93-2	1795	81.6	1.400	128 214	0.493	181	0.894	1.514	0.114	0.0129
C93-5	1795	81.6	1.451	123 708	3.619	167	0.751	1.549	0.098	0.0115
C93-6	1795	81.6	1.424	126 053	18.712	145	0.942	1.521	0.097	0.0102
C93-7	1795	81.6	1.363	131 695	1.585	170	0.977	1.469	0.106	0.0125
C93-8	1795	81.6	1.412	127 125	11.490	140	0.947	1.499	0.087	0.0099
C87-1	1668	75.8	1.183	140 997	3.193	131	0.971	1.254	0.071	0.0111
C87-2	1668	75.8	1.229	135 720	39.506	129	0.997	1.332	0.103	0.0105
C87-3	1668	75.8	1.355	123 100	72.915	128	0.982	1.442	0.087	0.0094
C87-5	1668	75.8	1.342	124 292	27.529	156	0.994	1.458	0.116	0.0116
C87-6	1697	77.1	1.311	129 443	36.358	108	0.987	1.385	0.074	0.0082
C87-7	1668	75.8	1.312	127 134	45.360	123	0.965	1.394	0.082	0.0094
C87-8	1697	77.1	1.265	134 150	53.200	160	0.992	1.371	0.106	0.0126
C82-1	1581	71.9	1.190	132 857	326 <sup>a</sup>	117	0.975	-	-	0.0098
C76-1	1469	66.8	1.087	135 143	255.317	121	0.967	1.164	0.077	0.0111
C72-1	1389	63.1	1.045	132 919	273.330	106	0.943	1.128	0.083	0.0101
C65-1	1260	57.3	0.930	135 484	326 <sup>a</sup>	91	0.892	-	-	0.0098
C50-1	961	43.7	0.887	108 343	74 <sup>a</sup>	104	0.987	-	-	0.0117
C40-1	770	35.0	0.645	119 380	74 <sup>a</sup>	74	0.975	-	-	0.0115
1.5 tonne ropes										
R91-1	1762	73.3	1.373	128 332	4.934	-	-	-	-	-
R91-2	1762	73.3	1.434	122 873	25.307	168	0.997	1.550	0.116	0.0117
R91-3	1762	73.3	1.414	124 611	3.453	180	0.998	1.510	0.096	0.0127
R91-4	1757	73.1	1.419	123 820	9.679	206	0.992	1.529	0.110	0.0146
R91-5	1757	73.1	1.405	125 053	17.302	152	0.994	1.497	0.092	0.0107
R91-6	1762	73.3	1.387	127 037	45.648	170	0.990	1.498	0.111	0.0121
R85-1	1629	67.8	1.353	120 399	35.274	174	0.989	1.471	0.118	0.0129
R85-2	1625	67.6	1.280	126 953	164.759	172	0.969	1.386	0.106	0.0134
R80-1	1540	64.1	1.211	127 168	580 <sup>a</sup>	148	0.978	-	-	0.0122
R30-1	588	24.5	0.468	125 641	141 <sup>a</sup>	71	0.947	-	-	0.0152

<sup>a</sup>Not failed.

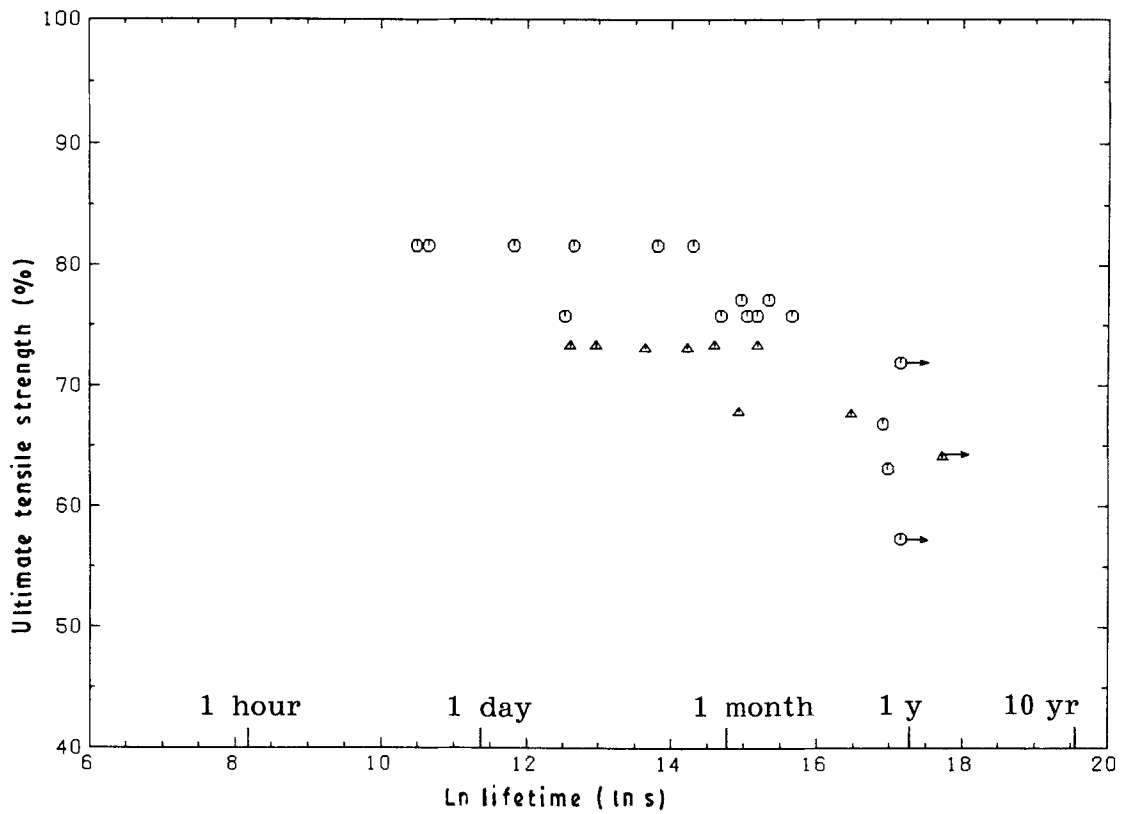


Figure 13 Applied stress versus lifetime, for (Δ) 1.5 tonne and (○) 3 tonne ropes. (→) Not failed.

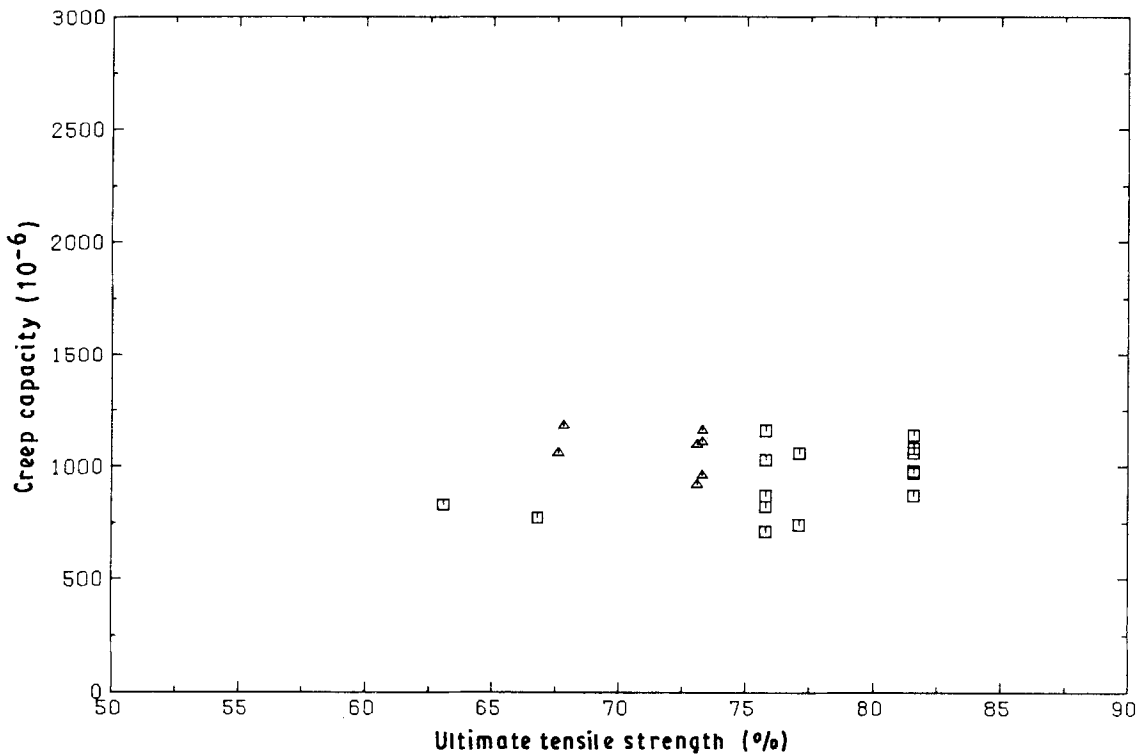


Figure 14 Creep capacity versus applied stress, for (Δ) 1.5 tonne and (○) 3 tonne ropes.

## 5.2. Creep prediction

An important feature of the creep behaviour of Kevlar 49 filaments reported by Ericksen [10] was the effect of the application and removal of an initial load. In multiple creep-recovery experiments, it was observed that the first creep curve had the highest slope, while those for subsequent curves were lower and all the

same (Fig. 18). The slopes of the subsequent curves were on average 60% of the initial values and this ratio was independent of stress level. Furthermore, it appeared that the length of the initial creep time did not influence the subsequent creep behaviour.

The comparison between the creep rate parameters,  $\beta$ , for Parafil and those for the initial creep of Kevlar

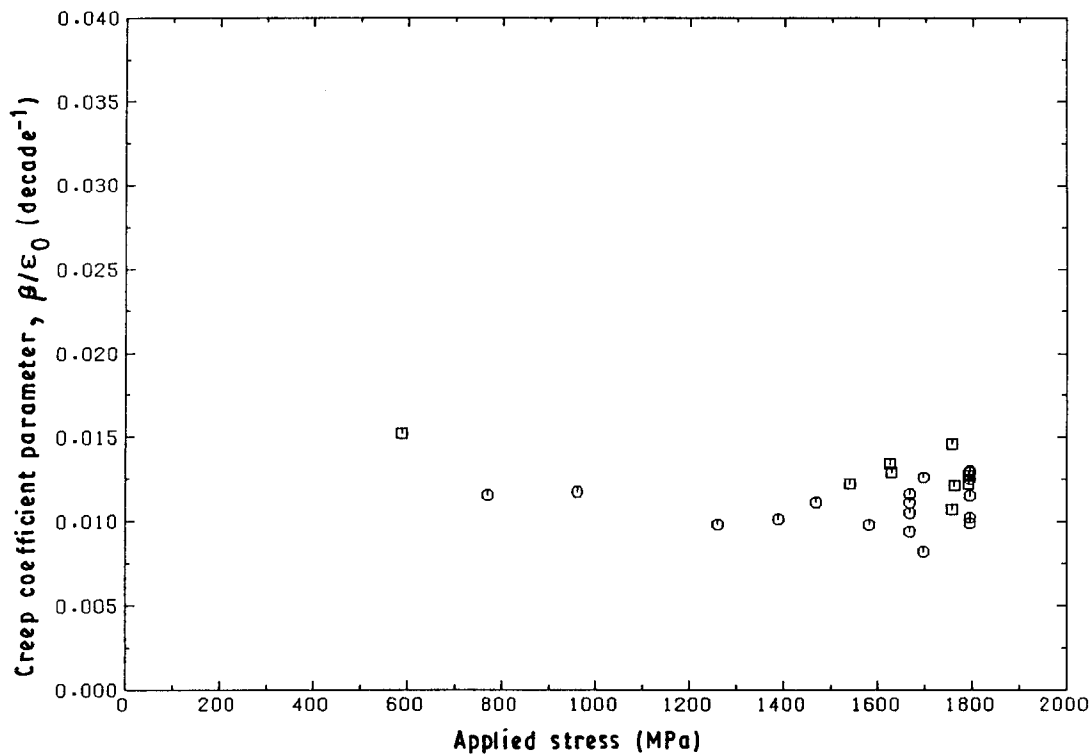


Figure 15 Stress dependence of the creep coefficient parameter, for ( $\Delta$ ) 1.5 tonne and ( $\circ$ ) 3 tonne ropes.

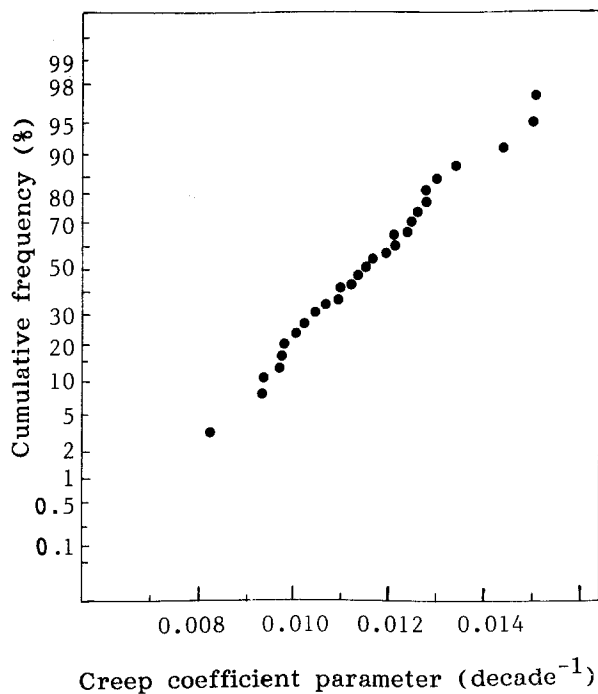


Figure 16 Normal distribution plot for the creep coefficient parameter.

49 filaments is shown in Fig. 19. Noting that the values measured here are associated with a second creep load, the disagreement shown in Fig. 19 should be expected. If the factor 60% is applied to the values of the creep rate parameter for filaments a better agreement will result. An important consequence of this experimental observation is that the pretensioning procedure has the effect of not only eliminating initial fibre disorientation within the ropes, but it seems to reduce creep and, probably, the related phenomenon, relaxation. Additional creep and relaxation tests on

pretensioned and non-pretensioned specimens are clearly necessary to quantify the conditioning effect for parallel-lay ropes, and are currently underway at a variety of locations. An understanding of this effect will be fundamental in major end uses where the application of the pretensioning load, as recommended by the manufacturer, would not be practical.

The conditioning effect is probably the best explanation for the high values for the creep rate parameters found by Chambers and Burgoyne [6] for 60 tonne NBL ropes. The high values observed for these ropes may be attributed to the fact that they were tested at loads varying from 68%–95% NBL while the pretensioning load was only 60% NBL.

The creep behaviour of single Kevlar 49 filaments over a period in excess of 4 years was studied by Walton and Majumdar [12]. The specimens were tested under three stress levels, 830, 1280 and 1830 MPa, at room temperature. The relationship between creep coefficient and elapsed time for each stress level was modelled by a power function

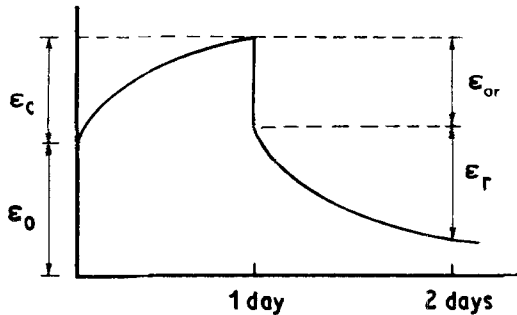
$$\phi(t) = At^n \quad (6)$$

where  $A$  and  $n$  are constants. For time  $t$  (h), the values found for  $A$  were 0.086 at 830 MPa, 0.062 at 1280 MPa and 0.055 at 1830 MPa, and  $n$  was found to have the same value, 0.086, for the three stress levels. These results show that the creep coefficient is stress dependent and increases as the applied stress decreases. It must be pointed out that only two specimens were tested for each stress level and, therefore, no indication on the scatter of the results was given.

A direct comparison between the equations found by Walton and Majumdar [12] and the creep coefficient for ropes given by Equation 5 would show that the values for the ropes would be less than those for

TABLE V Creep and recovery data. (Creep time = recovery time = 1 day)

Specimen	$\sigma$ (MPa)	Creep			Recovery				
		$\epsilon_0$ (%)	$\epsilon_c$ (%)	$\epsilon_0 + \epsilon_c$ (%)	$\epsilon_{or}$ (%)	$\epsilon_r$ (%)	$\epsilon_{or} + \epsilon_r$ (%)	$\epsilon_{or}/\epsilon_0$	$\epsilon_{or} + \epsilon_r/\epsilon_0 + \epsilon_c$
VR1	1368	1.069	0.049	1.118	1.041	0.068	1.109	0.97	0.99
VR2	1139	0.917	0.036	0.953	0.862	0.074	0.936	0.94	0.98
VR3	913	0.738	0.034	0.772	0.702	0.063	0.765	0.95	0.99



$\epsilon_0$  = initial strain  
 $\epsilon_c$  = creep strain  
 $\epsilon_{or}$  = initial strain recovery  
 (measured immediately  
 after load removal)  
 $\epsilon_r$  = creep recovery

TABLE VI Load/unload elastic modulus for creep/recovery

Stage	VR1		VR2		VR3	
	$\sigma$ (MPa)	$E$ (MPa)	$\sigma$ (MPa)	$E$ (MPa)	$\sigma$ (MPa)	$E$ (MPa)
1st (loading)	1368	127 970	1139	124 210	913	123 710
2nd (unloading)	1368	131 410	1139	132 130	913	130 060
3rd (loading)	1368	127 610	1139	127 830	913	129 050

TABLE VII Creep rate and recovery rate parameters for the 1.5 tonne specimens tested under varying loads

Specimen	Applied stress (MPa)	Creep		Recovery	
		$\beta$ ( $10^{-6}$ decade $^{-1}$ )	Correlation coefficient	$\beta$ ( $10^{-6}$ decade $^{-1}$ )	Correlation coefficient
VR1	1368	91	0.988	- 138	- 0.995
VR2	1139	64	0.972	- 153	- 0.996
VR3	913	63	0.983	- 131	- 0.995

the filaments. That is because the latter were not conditioned, i.e. the filaments were not subjected to a pretensioning load before the tests, like the rope specimens in the present investigation. A more realistic comparison can be made by multiplying Equation 6 by the factor 0.6, which accounts for the effect of conditioning as observed by Ericksen [10]. This comparison is made in Fig. 20 which shows that most of the portions of the curves for Kevlar 49 filaments are contained within the 5% and 95% confidence limits found for the parallel-lay ropes.

### 5.3. Creep recovery

Another feature of the creep behaviour of Kevlar 49 observed by Ericksen [10], in the multiple creep/re-

covery experiments mentioned in the previous section, was that all the recovery curves had about the same slopes in a semi-log plot; these were slightly less than those for the initial creep period (83%) and about 38% higher than the slopes of the curves for the subsequent creep periods. It was also found that the recovery rate parameter depends on stress in the same way as the creep rate parameter, with similar scatter.

The results found for the ropes are rather different. Table VII shows that the ratio between the recovery and creep parameters was higher than that observed by Ericksen [10]. It must be pointed out that the load/unloading rates were controlled in the experiments conducted by Ericksen [10] and, therefore, his results may be more realistic than those found here.

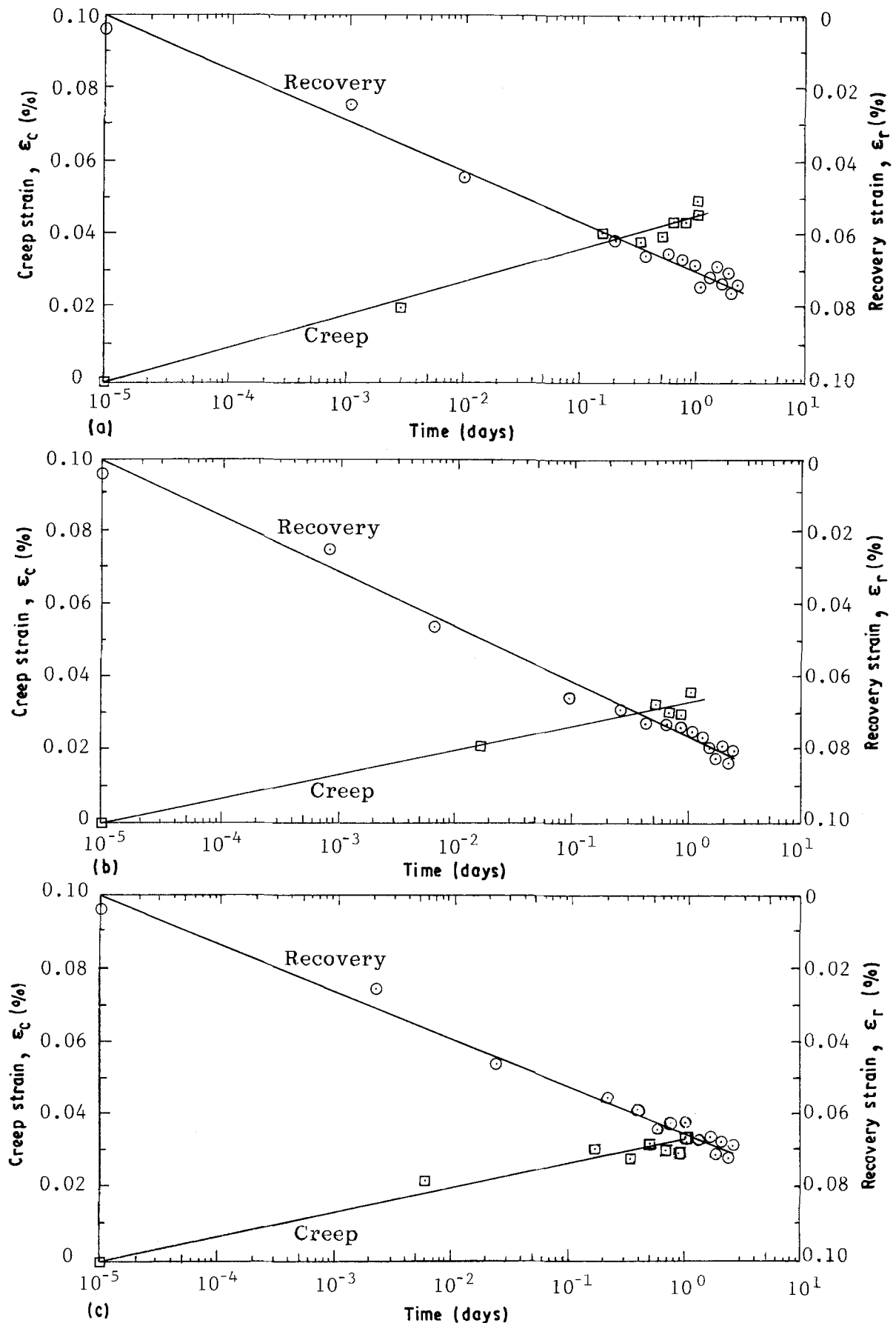


Figure 17 Creep and recovery at different stresses ( $\epsilon_c$  and  $\epsilon_r$ , as defined in Table V). (a) Specimen VR1, stress = 1368 MPa; (b) Specimen VR2, Stress = 1139 MPa; (c) Specimen VR3, stress = 913 MPa.

#### 5.4. Stress dependence of the creep behaviour

The degree of stress dependence of the creep behaviour of Kevlar 49 is still an unresolved point. Cook *et*

*al.* [7], Howard [8] and Ericksen [10] agree upon the logarithmic time law, but none of them went further to quantify the stress dependence of the creep coefficient.

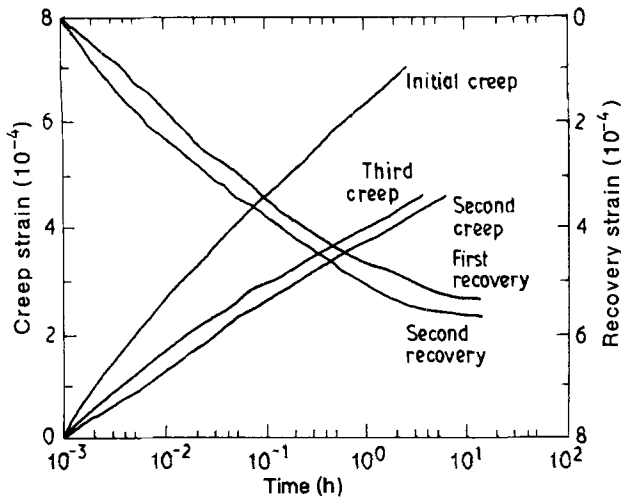


Figure 18 Repeated creep and recovery curves for Kevlar 49 filaments at room temperature. Creep load = 14.9 g [10].

Blades (quoted in Reference 11 reported that the total strain at time  $t$  may be estimated by the expression

$$\varepsilon(t) = \varepsilon_1 + \varepsilon_1 C \log_{10}(t) \quad (7)$$

where  $\varepsilon_1$  is the strain at unit time and  $C$  is a constant which was found to be 0.016 for Kevlar 49 and 0.024 for Kevlar 29. If the time  $t$  in the above equation is expressed in seconds, the strain,  $\varepsilon_1$ , may be considered as the initial strain and the constant,  $C$ , would be the creep coefficient parameter as defined in Equation 4. Thus, as in the present study, the creep coefficient for Kevlar was also assumed to be stress independent. The difference between the values 0.016 for Kevlar and 0.012 for the ropes might be explained by the conditioning effect mentioned in Section 5.2. Unfortunately no information is given in the paper by Schaeffgen [11] on this aspect of the test procedure.

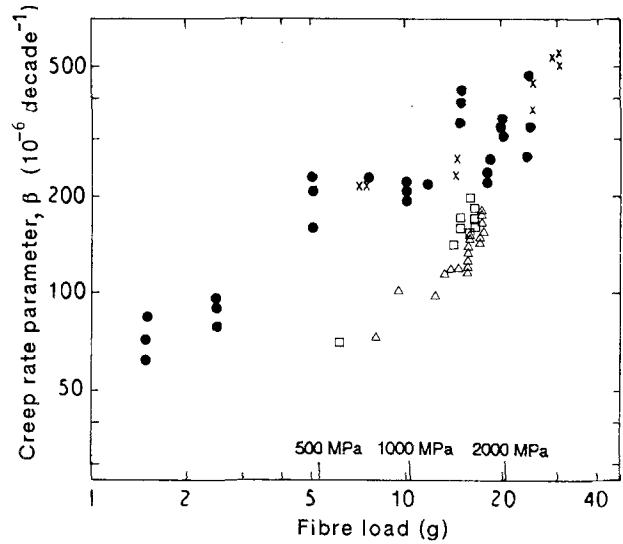


Figure 19 Log-log plot of creep rate parameter versus load, for (x, ●) Kevlar 49 non-conditioned filament specimens [10] and (□, △) conditioned Type G Parafil specimens. (x) LVDT measurements, (●) optical strain measurements, (□) 1.5 tonne ropes, (△) 3 tonne ropes.

The results reported by Walton and Majumdar [12], on the other hand, showed that the creep coefficient was stress dependent as already mentioned in Section 5.2.

## 6. Prediction of creep under varying load

The major consequence of the assumption that the creep coefficient, and so the creep compliance, is independent of stress, is the linearity of the viscoelastic behaviour of the material. Thus, the Boltzmann superposition principle can be applied to predict the creep

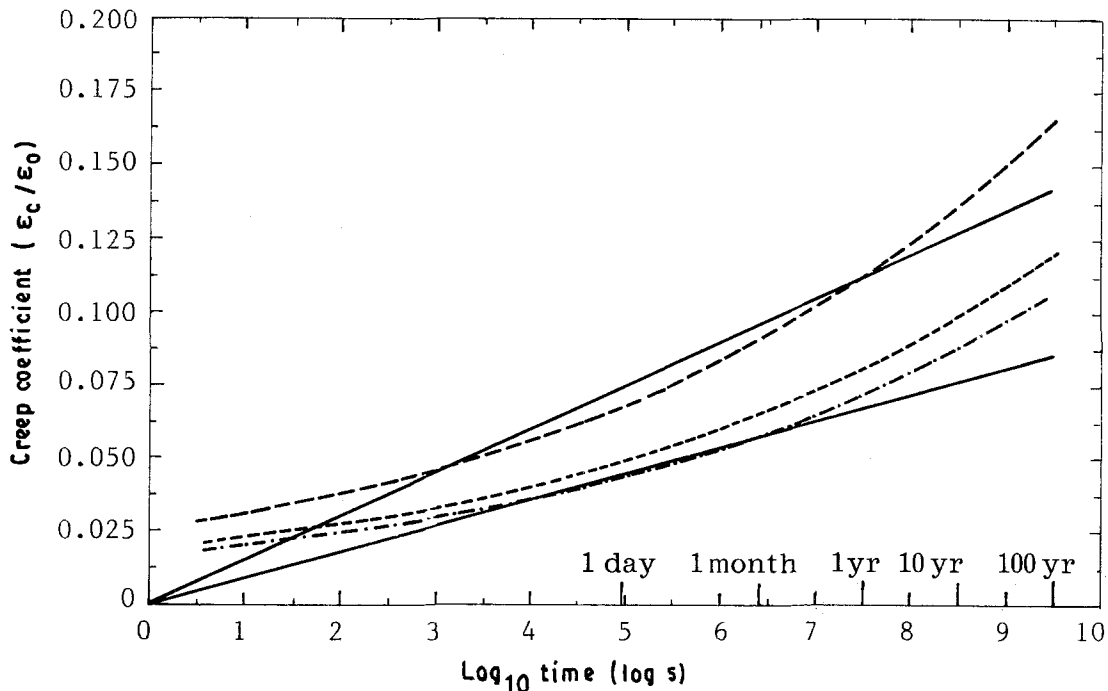


Figure 20 Comparison between the creep coefficients for Parafil and Kevlar filaments. The curves for filaments were plotted using the equations proposed by Walton and Majumdar [12] multiplied by 0.60 to account for the conditioning effect as observed by Ericksen [10]. (—) Type G parafil, 5% and 95% confidence limits. Kevlar 49 filaments, stress: (---) 830 MPa, (- - -) 1280 MPa, (— · —) 1830 MPa.

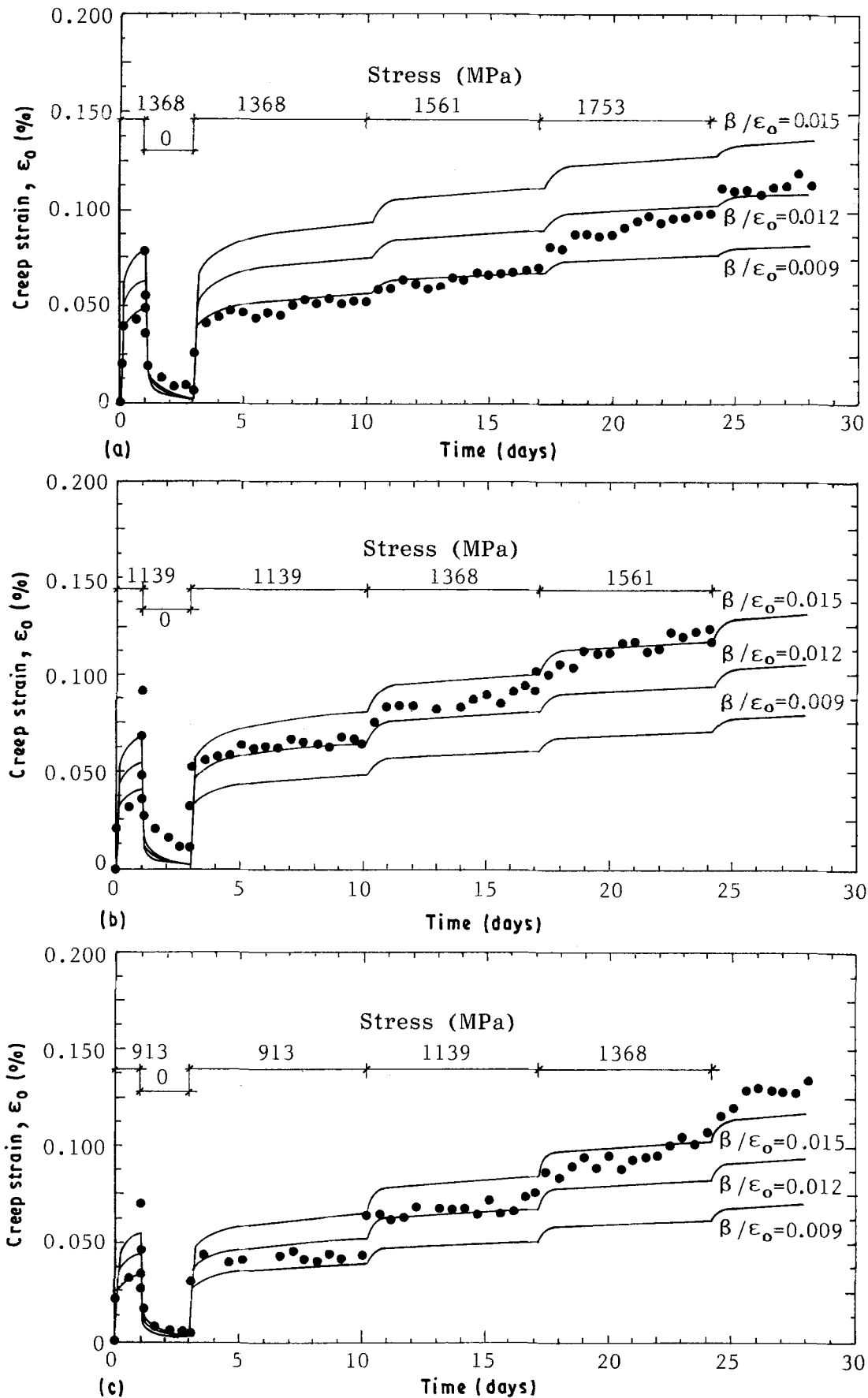


Figure 21 Comparison between (—) predicted and (●) observed creep strains of parallel-lay aramid ropes under varying loads, for (a) Specimen VR1, (b) Specimen VR2, (c) Specimen VR3.

behaviour under varying load. This principle states that (a) the creep strain is a function of the entire loading history, (b) each loading step makes an independent contribution to the final strain, and (c) the

final strain can be obtained by the simple addition of each contribution.

For a loading programme in which incremental stresses  $\Delta\sigma_1, \Delta\sigma_2, \Delta\sigma_3$ , etc, are added at times  $t_1, t_2, t_3$ ,



etc, the total strain at time,  $t$ , is obtained by

$$\begin{aligned} \varepsilon(t) = & \Delta\sigma_1 J(t - t_1) + \Delta\sigma_2 J(t - t_2) \\ & + \Delta\sigma_3 J(t - t_3) + \dots \end{aligned} \quad (8)$$

where  $J(t)$  is the creep compliance

$$J(t) = \varepsilon(t)/\sigma = [1 + \phi(t)]/E \quad (9)$$

The creep strain,  $\varepsilon_c(t) = \varepsilon(t) - \varepsilon_0$ , can be obtained by considering only the time-dependent term of the creep compliance  $[\phi(t)/E]$  in Equation 9. Thus

$$\begin{aligned} \varepsilon_c(t) = & [\Delta\sigma_1 \phi(t - t_1) + \Delta\sigma_2 \phi(t - t_2) \\ & + \Delta\sigma_3 \phi(t - t_3) + \dots]/E \end{aligned} \quad (10)$$

A comparison between the creep strain for specimens VR1, VR2 and VR3 (see Table III) and the creep strain values given by Equation 10 is shown in Fig. 21. The creep coefficient was obtained by

$$\phi(t - t_i) = (0.012 \pm 0.003) \log_{10}(t - t_i)/E \quad (11)$$

where  $E$  is the elastic modulus given in Table VI for the first loading stage, and the stress increments for each specimen were obtained from Fig. 4. Fig. 21 shows that the agreement between the experimental and predicted results is reasonable, given the uncertainty with which the creep coefficient was calculated.

## 7. Conclusions

The creep behaviour of Type G Parafil ropes at ambient temperature has been studied over a period of up to 580 days. The results of the experimental investigation conducted on ropes of 1.5 and 3.0 tonne nominal breaking loads has shown that:

1. creep and recovery in parallel-lay ropes can be adequately described using a logarithmic time law;
2. the creep rate at any time increases with stress;
3. a considerable scatter in the measured creep rate values was observed and this seems to be a characteristic of the material;
4. the creep coefficient for parallel-lay aramid ropes can be considered stress independent and estimated, with 90% certainty, by the expression  $\phi(t) = (0.012 \pm 0.003) \log_{10}(t)$ , where  $t$  is expressed in seconds;

5. the comparison between the creep rate values for parallel-lay ropes and Kevlar 49 fibres indicated that the application of a pretensioning load has the effect of reducing the creep strain of ropes in subsequent loading.

## Acknowledgements

This work is part of an on-going research programme on structural applications of Parafil ropes. This part of the research was sponsored by CNPq, Conselho Nacional de Desenvolvimento Científico e Tecnológico, Brazil, Linear Composites Ltd, UK, and the Science and Engineering Research Council, UK, as part of its COIN (Concrete Offshore in the Nineties) programme.

## References

1. J. J. CHAMBERS, PhD thesis, University of London (1986).
2. C. J. BURGOYNE, in "Proceedings of Symposium on Engineering Applications of Parafil Ropes", edited by C. J. Burgoyne, Imperial College, January 1988 (Imperial College) p. 39.
3. C. BAXTER, *ibid.*, p. 49.
4. M. M. SALAMA, *Marine Technol.* **21** (1984) 234.
5. G. B. GUIMARÃES and C. J. BURGOYNE, in "Life Prediction of a Parallel lay Aramid Rope", Report no. 02/91, Departamento de Engenharia Civil, PUC-Rio, October 1991, 22 pp.
6. J. J. CHAMBERS and C. J. BURGOYNE, *J. Mater. Sci.* **25** (1990) 3723.
7. J. COOK, A. HOWARD, N. J. PARRAT and K. D. POTTER, in "Proceedings of the 3rd Risø International Symposium on Metallurgy and Materials Science", edited by H. Lilholt and R. Talreja, (Risø National Laboratory, Roskilde, Denmark, 1982) p. 193.
8. A. HOWARD, in "TEQC Proceedings", University of Surrey, September 1983 (Butterworths, 1983) p. 264.
9. R. H. ERICKSEN, *Composites* July 7 (1976) 189.
10. *Idem*, *Polymer* **26** (1985) 733.
11. J. R. SCHAEFGEN, in "The Strength and Stiffness of Polymers", edited by A. E. Zachariades and R. S. Potter (Marcel Dekker, New York, 1983) p. 327.
12. P. L. WALTON and A. J. MAJUMDAR, *J. Mater. Sci.* **18** (1983) 2939.

Received 16 January  
and accepted 7 June 1991